

# Fusion-Based Event-Triggered $H_\infty$ State Estimation of Networked Autonomous Surface Vehicles With Measurement Outliers and Cyber-Attacks

Shen Yan<sup>ID</sup>, Zhou Gu<sup>ID</sup>, Senior Member, IEEE, Ju H. Park<sup>ID</sup>, Senior Member, IEEE, and Mouquan Shen<sup>ID</sup>

**Abstract**—This paper investigates the fusion-based event-triggered  $H_\infty$  state estimation of autonomous surface vehicles (ASVs) against measurement outliers and cyber-attacks. To release communication burden, a novel fusion-based event-triggered mechanism (FETM) dependent on the fusion of historical system outputs is proposed. There exist two advantages of this mechanism: 1) the use of fusion signal is able to avoid the information loss between two sampling instants and reduce the redundant triggering events resulted from system disturbances and noises; 2) by requiring the error signal in the triggering condition not only larger than a lower threshold but also less than an upper threshold, the false triggering events incurred by measurement outliers also can be discarded. Then, a time-varying delay system is established to represent the event-triggered  $H_\infty$  state estimation error system with network-induced delays. Then, sufficient conditions are deduced for solving  $H_\infty$  estimator gain and triggering matrix of FETM. Lastly, some simulation results are given to illustrate the merits of the theoretical method.

**Index Terms**—Fusion-based event-triggered mechanism, networked systems, autonomous surface vehicles, cyber-attacks, measurement outliers,  $H_\infty$  state estimation.

## I. INTRODUCTION

AS THE depletion of land resources, more and more interest and effort have been devoted exploring and utilizing marine resources like oil, natural gas, etc. Due to the features of good mobility, inexpensive cost and high intelligence, ASVs are able to work under harsh conditions to avoid personnel

Manuscript received 16 March 2022; revised 15 September 2022 and 15 March 2023; accepted 19 December 2023. Date of publication 17 January 2024; date of current version 2 July 2024. This work was supported in part by the National Natural Science Foundation of China under Grant 62103193, Grant 62273183, and Grant 62173177; and in part by the Natural Science Foundation of Jiangsu Province of China under Grant BK20200769 and Grant BK20231288. The work of Ju H. Park was supported by the National Research Foundation of Korea (NRF) funded by the Korean Government (Ministry of Science and Information and Communications Technology) under Grant 2019R1A5A8080290. The Associate Editor for this article was P. Pisu. (*Corresponding authors:* Zhou Gu; Ju H. Park.)

Shen Yan is with the College of Mechanical and Electronic Engineering, Nanjing Forestry University, Nanjing 210037, China (e-mail: yanshenzdh@gmail.com).

Zhou Gu is with the School of Electrical Engineering, Anhui Polytechnic University, Wuhu 241000, China, and also with the College of Mechanical and Electronic Engineering, Nanjing Forestry University, Nanjing 210037, China (e-mail: gzh1808@163.com).

Ju H. Park is with the Department of Electrical Engineering, Yeungnam University, Gyeongsan-si 38541, South Korea (e-mail: jessie@ynu.ac.kr).

Mouquan Shen is with the College of Electrical Engineering and Control Science, Nanjing Technology University, Nanjing 211816, China (e-mail: shenmouquan@njtech.edu.cn).

Digital Object Identifier 10.1109/TITS.2024.3350536

injury. In recent years, ASVs play an important role in the exploration of marine resources, environmental monitoring and rescuing [1], [2], [3], [4]. In particular, it is costly and difficult to measure the full state of real systems as the control input. Thus, the state estimation is a vital manner to estimate the state of ASVs by the measured output. Since the offshore tasks are carried out, signals are communicated over wireless network to control and operate the ASVs. For the state estimation of networked ASVs, it is unavoidable to be affected by the issues of limited bandwidth and network security.

To cope with the constraint of limited bandwidth, event-triggered scheme has been applied to alternate the conventional time-triggered strategy [5], [6], [7], [8]. In [9], a learning-based event-triggered path tracking control issue is addressed for ASVs, where an adjustable triggering threshold is introduced to regulate the data transmitting rate. [10] investigates a discrete-time event-triggered mechanism (ETM) for an ASV with transmission delays to increase the utilization of network bandwidth. The event-triggered cooperative control problem for networked ASVs is addressed in [11] to reduce unnecessary transmissions to save limited communication and computation resources. Because of some abrupt hits from waves and foreign body in the water, the sensors are easy to generate measurement outliers, the amplitude of which is usually much larger than the normal values. If the measurement outliers can not be tackled appropriately, they are inevitable to result in false triggers and deteriorate the estimation and control performance of ASVs. In order to solve this issue, a saturation-based approach is applied to restrain the impact of the measurement outliers on the state estimation for neural networks [12]. In contrast to the saturation-based approach in [12], actually, it is better to drop the measurement outliers directly. In [13], an outlier-resistant ETM (ORETM) is presented to distinguish the normal values and the outliers. In this scheme, the distinguished outliers will not be triggered and then be discarded directly. In addition, for networked ASVs, it is usually to be disturbed frequently by the fluctuations resulted from winds and waves. In such circumstances, the above ETMs in [9], [10], [11], and [13] using the current system states or outputs are sensitive to the disturbances or measurement noises, which could cause redundant transmissions and over-occupation of limited bandwidth. In terms of the negative effects of measurement outliers and frequent fluctuations in real environment, how to design an effective

ETM to discard the false triggering events incurred by outliers and redundant triggering events resulted from fluctuations is the first motivation of this work.

On the other research line, the security of communication channels is important for networked systems. When the data packets communicated among the network channels are attacked by adversaries, the system performance, even stability, will be deteriorated. For instance, the hacker launched the cyber-attack called StuxNet virus to invade a nuclear power station of Iranian, which causes the power failures to 60% users [14]. There are two typical types of cyber-attacks, the one is Denial-of-service (DoS) attack [16], [17], [18] and the other is deception attack [19], [20], [21]. Recently, much effort has been devoted to studying the issues of secure state estimation against cyber-attacks. Specifically, in [16], for the state estimation of networked systems, the measured signals are transmitted to a remote estimator via a multi-channel network, which are possible to be blocked by DoS attack. An distributed state estimation issue for networked systems with DoS attack is addressed in [17], where an observer-based ETM is developed to increase the efficiency of communication network. In contrast to DoS attack, deception attack is harder to be detected due to their stealthy and deceptive features. In [19], the security of state estimation issue is studied for networked systems under false data injection attacks, a kind of deception attacks, in which the network channels among the sensor and estimator are vulnerable to attacks launched by adversaries. Reference [20] is concerned with the design of event-triggered recursive state estimator for stochastic complex dynamical networks against both deception and DoS attacks. Nevertheless, rare attention has been paid for the investigation of event-triggered  $H_\infty$  state estimation problem of networked ASVs with both measurement outliers and deception attacks, which further motivates the current work.

This article focuses on the fusion-based event-triggered  $H_\infty$  state estimation issue of networked ASVs, the theoretical results of which lead to that the undesirable triggering events caused by measurement outliers and disturbances can be decreased by the presented FETM and the designed estimator is resilient to the deception attacks. The main contributions are summarized as:

#### A. A Novel FETM

utilizing the sampled data of the historical system information over a fixed interval and the upper bound of triggering error is presented for the first time. Compared with the existing ORETM in [13], the use of historical system information is helpful to avoid the information loss during the intersample period and further reduce unnecessary triggering events generated by stochastic fluctuations. In addition, unlike the normal ETM in [22] and the integral-based ETM in [23], an upper bound of the triggering error is added into the FETM, which is used to exclude the false triggered events caused by measurement outliers.

#### B. A United Model

of event-triggered  $H_\infty$  estimating error system of networked ASVs is formed as a time-varying delay system with the

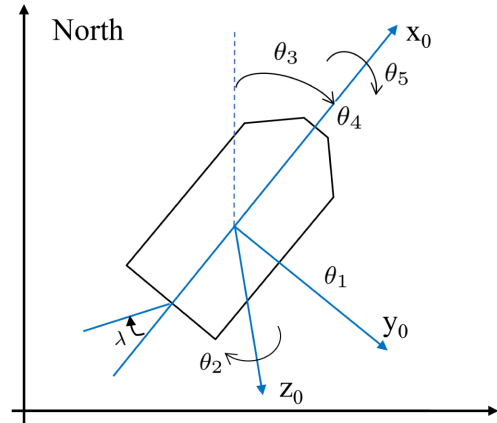


Fig. 1. Coordinate system for an ASV on the planar plane.

help of the Simpson's second rule to handle the time-varying integral term resulted from FETM. This model characterizes the impacts of the exogenous disturbances, communication delays, measurement outliers and deception attacks. Moreover, compared with the approximation method in [23], the Simpson's second rule could yield less approximation error.

#### C. A Co-Design Approach

is developed to solve the estimator gain and the triggering matrix by using the Lyapunov method and a separation technique in Lemma 1. Different from the existing approach requiring special structure in [24], a slack variable is introduced to remove the coupling among estimator gains and variable matrices, which is potential to obtain less conservative results.

The outline of this paper is provided as below. The preliminaries of modeling the event-triggered estimating error systems of networked ASVs with outliers and cyber-attacks is presented in Section II. Then the stability conditions and estimator design conditions are produced in Section III. Some simulation results are carried out in Section IV to show the merits of the developed strategy. In Section V, the conclusions and some future investigations are proposed.

#### D. Notation

$\mathbf{He}(W)$  means  $W^T + W$ .  $\mathbf{Sy}(U, V) \triangleq V^T U V$ . The omitted entries induced by symmetry in a matrix is represented by \*. Kronecker product is denoted by  $\otimes$ .  $\cup_{l=0}^p A_l$  means the union of sets  $\{A_0, \dots, A_l, \dots, A_p\}$ .

## II. PRELIMINARIES

In this paper, FETM-based state estimation for ASVs is investigated. The earth- and body-fixed coordinates of the ASV are presented in Fig. 1, where  $X_0$ ,  $Y_0$ , and  $Z_0$  mean the longitudinal axis, transverse axis, and normal axis, respectively; the roll, heading and rudder angle are represented by  $\theta_5$ ,  $\theta_3$ ,  $\lambda$ , respectively; the roll, yaw and sway velocity are denoted by  $\theta_4$ ,  $\theta_2$ ,  $\theta_1$ , respectively.

By applying Taylor expansion and Laplace transformation, and ignoring some hydrodynamic effects, the following

transfer functions for the motion are derived [3]:

$$\begin{cases} \theta_1(s) = \frac{\mathcal{M}_1}{1 + \mathcal{N}_1 s} \lambda(s), \\ \theta_3(s) = \frac{1}{(1 + \mathcal{N}_2 s)s} [\mathcal{M}_2 \lambda(s) + \mathcal{M}_3 \theta_1(s) + \omega_1(s)], \\ \theta_5(s) = \frac{v^2}{s^2 + 2\kappa vs + v^2} [\mathcal{M}_4 \lambda(s) + \mathcal{M}_5 \theta_1(s) + \omega_2(s)], \end{cases} \quad (1)$$

where  $\omega_1$  and  $\omega_2$  are external disturbances.  $\mathcal{M}_1, \mathcal{M}_2, \mathcal{M}_3, \mathcal{M}_4, \mathcal{M}_5$  are constant gains,  $\mathcal{N}_1$  and  $\mathcal{N}_2$  mean time constants,  $\kappa$  and  $v$  denote the damping ratio and the undamped natural frequency.

With the help of inverse Laplace transform, the dynamics of an ASV is accordingly formulated as follows [3], [23]:

$$\begin{cases} \dot{\theta}_1(t) = -\frac{1}{\mathcal{N}_1} \theta_1(t) + \frac{\mathcal{M}_1}{\mathcal{N}_1} \lambda(t), \\ \dot{\theta}_2(t) = \frac{\mathcal{M}_2}{\mathcal{N}_2} \theta_1(t) - \frac{1}{\mathcal{N}_2} \theta_2(t) + \frac{\mathcal{M}_3}{\mathcal{N}_2} \lambda(t) + \frac{1}{\mathcal{N}_2} w_1(t), \\ \dot{\theta}_3(t) = \theta_2(t), \\ \dot{\theta}_4(t) = v^2 \mathcal{M}_4 \theta_1(t) - 2\kappa v \theta_4(t) - v^2 \theta_5(t), \\ \quad + v^2 \mathcal{M}_5 \lambda(t) + v^2 w_2(t) \\ \dot{\theta}_5(t) = \theta_4(t). \end{cases} \quad (2)$$

Define  $\theta(t) = [\theta_1(t), \theta_2(t), \theta_3(t), \theta_4(t), \theta_5(t)]^\top \in \mathbb{R}^n$ ,  $\omega(t) = [\omega_1(t), \omega_2(t)]^\top \in \mathbb{R}^{n_w}$ ,  $u(t) = \lambda(t) \in \mathbb{R}^1$ , and the state-space model of the ASV is derived as:

$$\dot{\theta}(t) = \mathfrak{A}\theta(t) + \mathfrak{B}u(t) + Fw(t), \quad (3)$$

where

$$\mathfrak{A} = \begin{bmatrix} -\frac{1}{\mathcal{N}_1} & 0 & 0 & 0 & 0 \\ \frac{\mathcal{M}_2}{\mathcal{N}_2} & -\frac{1}{\mathcal{N}_2} & 0 & 0 & 0 \\ 0 & 1 & 0 & 0 & 0 \\ v^2 \mathcal{M}_4 & 0 & 0 & -2\kappa v & -v^2 \\ 0 & 0 & 0 & 1 & 0 \end{bmatrix}, \quad F = \begin{bmatrix} 0 & 0 \\ \frac{1}{\mathcal{N}_2} & 0 \\ 0 & 0 \\ 0 & v^2 \\ 0 & 0 \end{bmatrix},$$

$$\mathfrak{B} = \begin{bmatrix} \frac{\mathcal{M}_1}{\mathcal{N}_1} & \frac{\mathcal{M}_3}{\mathcal{N}_2} & 0 & v^2 \mathcal{M}_5 & 0 \end{bmatrix}^\top.$$

In this article, we suppose that the ASV is stabilized by a local feedback controller  $u(t) = \mathfrak{K}x(t)$ , and  $A = \mathfrak{A} + \mathfrak{B}\mathfrak{K}$  is Hurwitz. The closed-loop ASV system is presented as

$$\begin{cases} \dot{\theta}(t) = A\theta(t) + Fw(t) \\ v(t) = C\theta(t) \\ z(t) = D\theta(t) \end{cases}, \quad (4)$$

in which  $v(t) \in \mathbb{R}^{n_v}$  and  $z(t) \in \mathbb{R}^{n_z}$  means system output and performance output, respectively.

Considering the limitation of network bandwidth, an event-triggered communication mechanism is utilized to reduce data transmissions. Different from the traditional event-triggered filter design, the average value of historical outputs  $\bar{v}(t) = \frac{1}{\tau} \int_{t-\tau}^t v(s)ds$  is obtained by smart sensor. Then, the sampled data of  $\bar{v}(t)$ ,  $\bar{v}(p_k h) = \frac{1}{\tau} \int_{p_k h - \tau}^{p_k h} v(s)ds$  is utilized as the input of the following scheme:

$$\begin{aligned} t_{k+1} h = t_k h + \min_{l>0} \{lh | \delta_1 \mathbf{Sy}(\Psi, \bar{v}(t_k h)) \leq \mathbf{Sy}(\Psi, \epsilon(p_k h)) \\ \leq \delta_2 \mathbf{Sy}(\Psi, \bar{v}(t_k h))\}, \end{aligned} \quad (5)$$

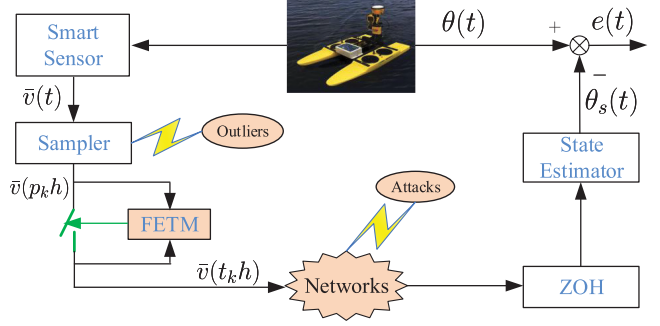


Fig. 2. The frame of state estimation for ASV under FETM.

where the sampling interval is shown by  $h$  and it is chosen to be smaller than the interval of the historical information  $\tau$ ;  $t_k h$  and  $t_{k+1} h$  represents the latest and next triggering instants, respectively;  $p_k h = t_k h + lh$  ( $l \in \mathbb{N}$ ) denotes the current sampling time;  $\epsilon(p_k h) = \bar{v}(p_k h) - \bar{v}(t_k h)$ ;  $\Psi > 0$  is the weighting matrix;  $\delta_1, \delta_2$  ( $0 < \delta_1 < \delta_2$ ) are the triggering threshold parameters. The framework of state estimation for a networked ASV with FETM is illustrated in Fig. 2. From this figure, one can see that the average signal  $\bar{v}(t)$  is derived by smart sensor, then it is sampled by the sampler as the input of FETM, which is constructed in (5) to reduce the undesirable triggering events. When the triggered data  $\bar{v}(t_k h)$  is transmitted over the network channel, an zero-order holder (ZOH) is utilized to keep the signal as  $\bar{v}(t_k h)$  until a new triggered data arrives. Then, a state estimator that is resilient to the deception attacks injected in triggered data is designed to estimate the system state.

*Remark 1:* When the interval  $\tau$  infinitely approach to 0, one can get  $\lim_{\tau \rightarrow 0} \frac{1}{\tau} \int_{t-\tau}^t v(s)ds = v(t)$ . As a result, the above FETM reduces to

$$\begin{aligned} t_{k+1} h = t_k h + \min_{l>0} \{lh | \delta_1 \mathbf{Sy}(\Psi, v(t_k h)) \leq \mathbf{Sy}(\Psi, \hat{v}(p_k h)) \\ \leq \delta_2 \mathbf{Sy}(\Psi, v(t_k h))\}, \end{aligned} \quad (6)$$

which is the existing ORETM in [13] with  $\hat{v}(p_k h) = v(p_k h) - v(t_k h)$ . In addition, if  $\delta_2 \rightarrow \infty$ , our FETM is further reduced as the following normal ETM [22]:

$$t_{k+1} h = t_k h + \min_{l>0} \{lh | \delta_1 \mathbf{Sy}(\Psi, v(t_k h)) \leq \mathbf{Sy}(\Psi, \hat{v}(p_k h))\}. \quad (7)$$

Compared with the schemes in [13] and [22] utilizing current information, our presented FETM in view of the average of historical outputs can avoid redundant triggered signals especially for the system with stochastic disturbances and noises.

*Remark 2:* The input of estimator using the conventional sampling manner losses the information during the consecutive sampling instants. To reduce such information loss, the fusion signal of historical outputs,  $\bar{v}(t) = \frac{1}{\tau} \int_{t-\tau}^t v(s)ds$ , instead of the instant signal  $v(t)$  is sampled as the estimator input. Additionally, with the aid of sampler, a positive inter-event time (sampling period  $h$ ) exists naturally and then Zeno behavior is avoided [25].

*Remark 3:* In the presented FETM, there exist two scalars  $\delta_1, \delta_2$  satisfying  $0 < \delta_1 < \delta_2$  and a variable matrix  $\Psi$ . The values of  $\delta_1$  and  $\delta_2$  affect the filter level of the FETM, particularly,  $\delta_1$  is used to determine the “unnecessary” data and  $\delta_2$  accounts for identifying the measurement outliers.

The signal transmitted to the estimator is expressed as

$$\hat{v}(t) = \bar{v}(t_k h) = \bar{v}(p_k h) - \epsilon(p_k h), \quad (8)$$

for  $t \in \Lambda \triangleq [t_k h + \eta_k, t_{k+1} h + \eta_{k+1}]$ , where  $\eta_k$  is the communication delay with upper bound  $\bar{\eta}$ .

For  $t \in \Lambda_l \triangleq [t_k h + l h + \vartheta_l, t_k h + (l+1)h + \vartheta_{l+1}]$  with  $\vartheta_0 = \eta_k$ ,  $\vartheta_{t_{k+1}-t_k} = \eta_{k+1}$ ,  $\vartheta_l \leq \bar{\eta}$  and  $\Lambda = \cup_{l=0}^{t_{k+1}-t_k} \Lambda_l$ , define  $\eta(t) \triangleq t - p_k h$  and it satisfies  $0 \leq \eta(t) \leq h + \bar{\eta} \triangleq \eta_M$ . Based on this definition and the consideration of deception attacks,  $\hat{v}(t)$  is further modified as

$$\hat{v}_a(t) = \frac{1}{\tau} \int_{t-\eta(t)-\tau}^{t-\eta(t)} v(s) ds - \epsilon(p_k h) + \beta(t) g(v(t - \eta(t))), \quad (9)$$

where  $\beta(t)$  is a stochastic variable obeying the Bernoulli distribution,  $\mathbb{E}\{\beta(t)\} = \beta$  means the probability of attack launching. Additionally, the deception attack signal  $g(v(t))$  is supposed to satisfy

$$\|g(v(t))\|_2 \leq \|GCx(t)\|_2, \quad (10)$$

in which the matrix  $G$  represents the upper bound of attack signal. To handle the deception attacks, this condition will be utilized to obtain the stability analysis and estimator design conditions in Theorem 1 and Theorem 2.

Defining  $d(t) \triangleq \eta(t) + \tau$ ,  $\tau \leq d(t) \leq d_M \triangleq \eta_M + \tau$ , one has

$$\bar{v}(p_k h) = \frac{1}{\tau} \int_{t-d(t)}^{t-\eta(t)} v(s) ds. \quad (11)$$

According to the Simpson's second rule [26], the time-varying distributed term in (11) can be approximated as

$$\begin{aligned} \bar{v}(p_k h) &\approx \frac{1}{8} [v(t - \eta(t)) + 3v(t - \eta(t) - \tau/3) \\ &+ 3v(t - \eta(t) - 2\tau/3) + v(t - \eta(t) - \tau)]. \end{aligned} \quad (12)$$

*Remark 4:* In [23], the Simpson's rule:

$$\begin{aligned} \frac{1}{\tau} \int_{t-d(t)}^{t-\eta(t)} v(s) ds &\approx \frac{1}{6} [v(t - \eta(t) - \tau) \\ &+ 4v(t - \eta(t) - \tau/2) + v(t - \eta(t))] \end{aligned} \quad (13)$$

is used to cope with the integral term  $\frac{1}{\tau} \int_{t-d(t)}^{t-\eta(t)} v(s) ds$ , which yields an approximation error  $-\frac{\tau^5}{2880} |v(t-a)|$  for  $a \in [t-d(t), t-\eta(t)]$ . Note that our used Simpson's second rule leads to an error  $-\frac{\tau^5}{6480} |v(t-a)|$ , which is about half of the error induced by the method in [23].

By applying the signal  $\hat{v}_a(t)$ , the estimator to estimate the system state is formed as

$$\begin{cases} \dot{\theta}_s(t) = A\theta_s(t) + L_s(\hat{v}_a(t) - v_s(t)) \\ v_s(t) = C\theta_s(t) \end{cases}, \quad (14)$$

where  $\theta_s(t) \in \mathbb{R}^5$  is the state of estimator,  $v_s(t)$  means the output of the estimator and the estimator gain  $L_s$  needs to be determined.

Then, by substituting (9) and (12) into (14) and combining them with (4), the augmented estimating error system is established as

$$\begin{cases} \dot{\zeta}(t) = \mathbb{A}\zeta(t) + \mathbb{F}w(t) - \mathbb{B} \sum_{j=0}^3 f_j \zeta(t - d_j(t)) \\ \quad - \beta(t) \mathbb{B}_g g(v(t - \eta(t))) + \mathbb{B}_\epsilon \epsilon(p_k h) \\ z(t) = \mathbb{D}\zeta(t), \end{cases}, \quad (15)$$

where  $\zeta(t) = [\theta^\top(t) \ e^\top(t)]^\top$ ,  $e(t) = \theta(t) - \theta_s(t)$ ,  $d_j(t) = \eta(t) + j\tau/3$ ,  $d_{Mj} = \eta_M + j\tau/3$ ,  $f_0 = 1/8$ ,  $f_1 = 3/8$ ,  $f_2 = 3/8$ ,  $f_3 = 1/8$ , and

$$\begin{aligned} \mathbb{A} &= \begin{bmatrix} A & 0 \\ L_s C & A - L_s C \end{bmatrix}, \mathbb{B} = \begin{bmatrix} 0 & 0 \\ L_s C & 0 \end{bmatrix}, \\ \mathbb{B}_\epsilon &= \mathbb{B}_g = \begin{bmatrix} 0 \\ L_s \end{bmatrix}, \mathbb{F} = \begin{bmatrix} F \\ F \end{bmatrix}, \mathbb{D} = \begin{bmatrix} D & 0 \end{bmatrix}. \end{aligned}$$

Our purpose is to obtain a fusion-based event-triggered  $H_\infty$  estimator (14) such that the estimating error system (15) is mean-square asymptotically stable with a given  $H_\infty$  index  $\gamma > 0$ . To achieve this purpose, the next lemma is recalled.

*Lemma 1:* [27]  $\mathcal{X}_1 + \mathbf{He}(\mathcal{X}_2 \mathcal{X}_3) < 0$  can be deduced through the condition (16):

$$\begin{bmatrix} \mathcal{X}_1 + \mathbf{He}(\mathcal{X}_4 \mathcal{X}_3) & * \\ \mathcal{X}_2^\top - \mathcal{X}_4^\top + \mathcal{X}_5 \mathcal{X}_3 - \mathbf{He}(\mathcal{X}_5) \end{bmatrix} < 0. \quad (16)$$

### III. MAIN RESULTS

In this section, the system stability and estimator design of fusion-based event-triggered ASVs will be presented.

*Theorem 1:* For given  $\tau$ ,  $\delta_1$ ,  $\delta_2$ ,  $\beta$ ,  $\bar{\eta}$ ,  $h$  and estimation matrix  $L_s$ , the system (15) under the FETM (5) is asymptotically stable in mean-square sense and meets the  $H_\infty$  disturbance attenuation level  $\gamma$ , if there exist  $S_j > 0$ ,  $T_j > 0$  ( $j = 0, 1, 2, 3$ ),  $\Psi > 0$ ,  $W > 0$ ,  $\mathbf{N}$ , and  $U_j$  meeting  $\mathcal{T}_j > 0$ , such that

$$\Theta < 0, \quad (17)$$

where

$$\begin{aligned} \Theta &= \Upsilon + \mathbf{He}(\mathcal{N}\mathcal{G}), \\ \Upsilon &= \mathbf{He}\left(\mathbb{L}_2^\top W \mathbb{L}_1\right) + \mathbf{He}\left(\mathbb{L}_{13}^\top \mathbb{D} \mathbb{L}_2\right) \\ &\quad + \rho_1 \delta_1 \mathbf{Sy}\left(\Psi, \mathcal{H}\right) - \rho_1 \mathbf{Sy}(\Psi, \mathbb{L}_{11}) \\ &\quad + \rho_2 \mathbf{Sy}(\Psi, \mathbb{L}_{11}) - \rho_2 \delta_2 \mathbf{Sy}\left(\Psi, \mathcal{H}\right) \\ &\quad + \rho_3 \mathbf{Sy}\left(G^\top G, C \mathcal{J} \mathbb{L}_2\right) - \rho_3 \mathbf{Sy}(I, \mathbb{L}_{14}) \\ &\quad + \sum_{j=0}^3 d_{Mj} \mathbf{Sy}(T_j, \mathbb{L}_1) + \sum_{j=0}^3 \mathbf{Sy}(S_j, \mathbb{L}_2) \\ &\quad - \sum_{j=0}^3 \mathbf{Sy}(S_j, \mathbb{L}_{7+j}) - \sum_{j=0}^3 \frac{1}{d_{Mj}} \mathbf{Sy}(\mathcal{T}_j, \mathbf{L}) \\ &\quad - \gamma^2 \mathbf{Sy}(I_p, \mathbb{L}_{12}) - \mathbf{Sy}(I_q, \mathbb{L}_{13}), \end{aligned}$$

$$\begin{aligned}\mathcal{T}_j &= \begin{bmatrix} T_j & U_j \\ U_j & T_j \end{bmatrix}, \quad \mathbf{L} = \begin{bmatrix} \mathbb{L}_2 - \mathbb{L}_{3+j} \\ \mathbb{L}_{3+j} - \mathbb{L}_{7+j} \end{bmatrix}, \\ \mathcal{H} &= C\mathcal{I} \sum_{j=0}^3 f_j \mathbb{L}_{3+j} - \mathbb{L}_{11}, \quad \mathcal{I} = [I \ 0], \\ \mathcal{N} &= \mathbb{L}_1^\top \mathbf{N} + \alpha \mathbb{L}_2^\top \mathbf{N}, \\ \mathcal{G} &= -\mathbb{L}_1 + \mathbb{A}\mathbb{L}_2 + \mathbb{B} \sum_{j=0}^3 f_j \mathbb{L}_{3+j} \\ &\quad - \mathbb{B}_\epsilon \mathbb{L}_{11} + \mathbb{F}\mathbb{L}_{12} - \beta \mathbb{B}_g \mathbb{L}_{14}, \\ \mathbb{L}_a &\triangleq \begin{cases} \begin{bmatrix} 0_{2n,2na} & I_{2n} & 0_{2n,2n(10-a)+n_v+n_w+n_z+n_v} \\ 0_{n_v,2n \times 10} & I_{n_v} & 0_{n_v,n_w+n_z+n_v} \end{bmatrix}, & a=1, \dots, 10 \\ \begin{bmatrix} 0_{n_w,2n \times 10+n_v} & I_{n_w} & 0_{n_w,n_z+n_v} \end{bmatrix}, & a=11 \\ \begin{bmatrix} 0_{n_z,2n \times 10+n_v+n_w} & I_{n_z} & 0_{n_z,n_v} \end{bmatrix}, & a=12 \\ \begin{bmatrix} 0_{n_v,2n \times 10+n_v+n_w+n_z} & I_{n_v} \end{bmatrix}, & a=13 \\ \begin{bmatrix} 0_{n_v,2n \times 10+n_v+n_w+n_z} & I_{n_v} \end{bmatrix}, & a=14. \end{cases}\end{aligned}$$

Thus, the gain of state estimator is solved via  $L_s = N_2^{-1} \mathcal{L}_s$ .

*Proof.* The Lyapunov-Krasovskii functional is chosen as

$$V(t) = V_1(t) + V_2(t) + V_3(t), \quad (18)$$

where

$$\begin{aligned}V_1(t) &= \mathbf{Sy}(W, \varsigma(t)), \\ V_2(t) &= \sum_{j=0}^3 \int_{t-d_{Mj}}^t \mathbf{Sy}(S_j, \varsigma(s)) ds \\ V_3(t) &= \sum_{j=0}^3 \int_{d_{Mj}}^0 \int_{t-s}^t \mathbf{Sy}(T_j, \dot{\varsigma}(v)) dv ds.\end{aligned}$$

We calculate  $\dot{V}(t) = \sum_{i=1}^3 \dot{V}_i(t)$  as

$$\dot{V}_1(t) = 2\varsigma^\top(t) W \dot{\varsigma}(t), \quad (19)$$

$$\dot{V}_2(t) = \sum_{j=0}^3 \mathbf{Sy}(S_j, \varsigma(t)) - \sum_{j=0}^3 \mathbf{Sy}(S_j, \varsigma(t-d_{Mj})), \quad (20)$$

$$\begin{aligned}\dot{V}_3(t) &= \sum_{j=0}^3 d_{Mj} \mathbf{Sy}(T_j, \dot{\varsigma}(t)) \\ &\quad - \sum_{j=0}^3 \int_{t-d_{Mj}}^t \mathbf{Sy}(T_j, \dot{\varsigma}(s)) ds.\end{aligned} \quad (21)$$

By applying Jensen inequality combined with reciprocally convex technique in [28], it yields

$$-\sum_{j=0}^3 \int_{t-d_{Mj}}^t \mathbf{Sy}(T_j, \dot{\varsigma}(s)) ds \leq -\sum_{j=0}^3 \frac{1}{d_{Mj}} \mathbf{Sy}(\mathcal{T}_j, \zeta_j(t)), \quad (22)$$

$$\text{where } \zeta_j(t) = \begin{bmatrix} \varsigma(t) - \varsigma(t-d_j(t)) \\ \varsigma(t-d_j(t)) - \varsigma(t-d_{Mj}) \end{bmatrix}.$$

Define

$$\begin{aligned}\varphi(t) &= [\dot{\varsigma}^\top(t), \ \varsigma^\top(t), \ \varsigma_d^\top(t), \ \varsigma_{d_M}^\top(t), \\ &\quad \epsilon^\top(p_k h), \ w^\top(t), \ z^\top(t), \ g^\top(v(t-\eta(t)))]^\top\end{aligned} \quad (23)$$

with

$$\begin{aligned}\varsigma_d(t) &= [\varsigma^\top(t-d_0(t)), \ \varsigma^\top(t-d_1(t)), \ \varsigma^\top(t-d_2(t)), \ \varsigma^\top(t-d_3(t))]^\top, \\ \varsigma_{d_M}(t) &= [\varsigma^\top(t-d_{M0}), \ \varsigma^\top(t-d_{M1}), \ \varsigma^\top(t-d_{M2}), \ \varsigma^\top(t-d_{M3})]^\top.\end{aligned}$$

To guarantee the asymptotic stability of the estimating error system (15) with given  $H_\infty$  index, one requires that

$$\mathcal{O}(t) \triangleq \dot{V}(t) + z^\top(t) z(t) - \gamma^2 w^\top(t) w(t) < 0. \quad (24)$$

Combining (5) and (12), one can get

$$\begin{aligned}\delta_1 \mathbf{Sy}(\Psi, C\mathcal{I} \sum_{j=0}^3 f_j \varsigma(t-d_j(t))) \\ - \mathbf{Sy}(\Psi, \epsilon(p_k h)) > 0,\end{aligned} \quad (25)$$

$$\begin{aligned}\mathbf{Sy}(\Psi, \epsilon(p_k h)) \\ - \delta_2 \mathbf{Sy}(\Psi, C\mathcal{I} \sum_{j=0}^3 f_j \varsigma(t-d_j(t))) > 0,\end{aligned} \quad (26)$$

which can be reformed as

$$\rho_1 \delta_1 \mathbf{Sy}(\Psi, \mathcal{H}\varphi(t)) - \rho_1 \mathbf{Sy}(\Psi, \mathbb{L}_9 \varphi(t)) > 0, \quad (27)$$

$$\rho_2 \mathbf{Sy}(\Psi, \mathbb{L}_9 \varphi(t)) - \rho_2 \delta_2 \mathbf{Sy}(\Psi, \mathcal{H}\varphi(t)) > 0, \quad (28)$$

where  $\rho_1$  and  $\rho_2$  are two positive scalars.

According to the description of deception attacks  $g(v(t-\eta(t)))$  in (10), it yields

$$\rho_3 \mathbf{Sy}(G^\top G, C\mathcal{I} \mathbb{L}_2 \varphi(t)) - \rho_3 \mathbf{Sy}(I, \mathbb{L}_{12} \varphi(t)) > 0, \quad (29)$$

where  $\rho_3 > 0$  is a constant.

Then we have

$$\begin{aligned}\mathcal{O}(t) + \rho_1 \delta_1 \mathbf{Sy}(\Psi, \mathcal{H}\varphi(t)) - \rho_1 \mathbf{Sy}(\Psi, \mathbb{L}_9 \varphi(t)) \\ + \rho_2 \mathbf{Sy}(\Psi, \mathbb{L}_9 \varphi(t)) - \rho_2 \delta_2 \mathbf{Sy}(\Psi, \mathcal{H}\varphi(t)) \\ + \rho_3 \mathbf{Sy}(G^\top G, C\mathcal{I} \mathbb{L}_2 \varphi(t)) - \rho_3 \mathbf{Sy}(I, \mathbb{L}_{12} \varphi(t)) \\ \leq \mathbf{Sy}(\Upsilon, \varphi(t)),\end{aligned} \quad (30)$$

which guarantees that (24) holds if  $\mathbf{Sy}(\Upsilon, \varphi(t)) < 0$ .

From the definition of  $\varphi(t)$ , it leads to

$$\dot{\varphi}(t) = \mathbb{L}_1 \varphi(t), \quad \varphi(t) = \mathbb{L}_2 \varphi(t), \quad \mathbb{E}\{\mathbb{G}\varphi(t)\} = 0, \quad (31)$$

where  $\mathbb{G} = -\mathbb{L}_1 + \mathbb{A}\mathbb{L}_2 + \mathbb{B} \sum_{j=0}^3 f_j \mathbb{L}_{3+j} - \mathbb{B}_\epsilon \mathbb{L}_9 + \mathbb{F}\mathbb{L}_{10} - \beta(t) \mathbb{B}_g \mathbb{L}_{12}$ .

By constructing  $\mathcal{N} = \mathbb{L}_1^\top \mathbf{N} + \alpha \mathbb{L}_2^\top \mathbf{N}$ , it yields

$$\mathbb{E}\{\mathbf{Sy}(\Upsilon + \mathbf{He}(\mathcal{N}\mathbb{G}), \varphi(t))\} < 0, \quad (32)$$

According to  $\mathbb{E}\{\beta(t)\} = \beta$ , it is equivalent to

$$\Upsilon + \mathbf{He}(\mathcal{N}\mathbb{G}) < 0. \quad (33)$$

On the basis of (17), the condition (33) is satisfied to guarantee  $\mathbb{E}\{\mathcal{O}(t)\} < 0$ .

Then,  $\mathbb{E}\{\mathcal{O}(t)\} < 0$  leads to

$$\mathbb{E}\{\dot{V}(t)\} < -\mathbb{E}\{z^\top(t)z(t)\} + \gamma^2\mathbb{E}\{w^\top(t)w(t)\}. \quad (34)$$

According to (34), it gives

$$\begin{aligned} &\mathbb{E}\{V(\infty) - V(0)\} \\ &< \mathbb{E}\left\{\int_0^\infty (\gamma^2 w^\top(t)w(t) - z^\top(t)z(t)) dt\right\}. \end{aligned} \quad (35)$$

When  $w(t)$  is zero, it is derived that  $\mathbb{E}\{\dot{V}(t)\} < 0$  from (34), which implies the estimating error system (15) is asymptotically stable in mean-square sense. When  $w(t) \neq 0$  and  $x(0) = 0$ , the  $H_\infty$  level  $\gamma$  is ensured by  $\mathbb{E}\{\int_0^\infty z^\top(t)z(t)dt\} \leq \gamma^2\mathbb{E}\{\int_0^\infty w^\top(t)w(t)dt\}$  based on (35). These fulfill the proof. ■

*Theorem 2:* For given  $\tau$ ,  $\delta_1$ ,  $\delta_2$ ,  $\alpha$ ,  $\beta$ ,  $\bar{\eta}$ ,  $h$  and  $\mu$ , the system (15) under the METS (5) is asymptotically stable in mean-square sense and meets the  $H_\infty$  disturbance attenuation level  $\gamma$ , if there exist  $S_j > 0$ ,  $T_j > 0$  ( $j = 0, 1, 2, 3$ ),  $\Psi > 0$ ,  $W > 0$ ,  $N_1$ ,  $N_2$ ,  $N_3$ ,  $N_4$ ,  $X$ ,  $\mathcal{L}_s$  and  $U_j$  meeting  $\mathcal{T}_j > 0$ , such that

$$\hat{\Theta} < 0, \quad (36)$$

where

$$\begin{aligned} \hat{\Theta} &= \begin{bmatrix} \Upsilon + \mathbf{He}(\hat{\mathcal{N}}(\hat{\mathcal{G}} + \mathbb{A}_{\mathcal{G}})) & \hat{\mathcal{N}}\bar{\mathbb{A}}_2 + \mu\mathbb{A}_{\mathcal{G}}^\top \\ * & -\mu\mathbf{He}(\bar{\mathbb{A}}_1) \end{bmatrix}, \\ \hat{\mathcal{N}} &= \mathbb{L}_1^\top + \alpha\mathbb{L}_2^\top, \\ \hat{\mathcal{G}} &= -\mathbf{NL}_1 + \bar{\mathbb{A}}\mathbb{L}_2 + \hat{\mathbb{F}}\mathbb{L}_{12}, \\ \mathbb{A}_{\mathcal{G}} &= \hat{\bar{\mathbb{A}}}\mathbb{L}_2 - \hat{\bar{\mathbb{B}}} \sum_{j=0}^3 f_j \mathbb{L}_{3+j} + \hat{\bar{\mathbb{B}}}_\epsilon \mathbb{L}_{11} - \beta \hat{\bar{\mathbb{B}}}_g \mathbb{L}_{13}, \\ \mathbb{A}_{\mathcal{G}} &= \hat{\bar{\mathbb{A}}}\mathbb{L}_2 - \hat{\bar{\mathbb{B}}} \sum_{j=0}^3 f_j \mathbb{L}_{3+j} + \hat{\bar{\mathbb{B}}}_\epsilon \mathbb{L}_{11} - \beta \hat{\bar{\mathbb{B}}}_g \mathbb{L}_{13}, \\ \hat{\bar{\mathbb{A}}} &= \begin{bmatrix} N_1 A & N_2 A \\ N_3 A & N_4 A \end{bmatrix}, \quad \hat{\bar{\mathbb{A}}} = \begin{bmatrix} \mathcal{L}_s C & \mathcal{L}_s C \\ \mathcal{L}_s C & \mathcal{L}_s C \end{bmatrix}, \\ \bar{\mathbb{A}}_1 &= \begin{bmatrix} X & 0 \\ 0 & X \end{bmatrix}, \quad \bar{\mathbb{A}}_2 = \begin{bmatrix} N_2 - X & 0 \\ 0 & N_4 - X \end{bmatrix}, \\ \hat{\bar{\mathbb{B}}} &= \begin{bmatrix} \mathcal{L}_s C & 0 \\ \mathcal{L}_s C & 0 \end{bmatrix}, \quad \hat{\bar{\mathbb{B}}}_\epsilon = \hat{\bar{\mathbb{B}}}_g = \begin{bmatrix} \mathcal{L}_s \\ \mathcal{L}_s \end{bmatrix}, \quad \hat{\mathbb{F}} = \begin{bmatrix} (N_1 + N_2)F \\ (N_3 + N_4)F \end{bmatrix}. \end{aligned}$$

Furthermore, the gain of estimator can be solved via  $L_s = X^{-1}\mathcal{L}_s$ .

**Proof.** By choosing  $\mathbf{N} = \begin{bmatrix} N_1 & N_2 \\ N_3 & N_4 \end{bmatrix}$ , it yields

$$\mathbb{E}\{\mathbf{Sy}(\Upsilon + \mathbf{He}(\hat{\mathcal{N}}(\hat{\mathcal{G}} + \tilde{\mathcal{G}})), \varphi(t))\} < 0. \quad (37)$$

where

$$\begin{aligned} \tilde{\mathcal{G}} &= \bar{\mathbb{A}}\mathbb{L}_2 - \hat{\bar{\mathbb{B}}} \sum_{j=0}^3 f_j \mathbb{L}_{3+j} + \hat{\bar{\mathbb{B}}}_\epsilon \mathbb{L}_{11} - \beta \hat{\bar{\mathbb{B}}}_g \mathbb{L}_{13}, \\ \bar{\mathbb{A}} &= \begin{bmatrix} N_2 L_s C & N_2 L_s C \\ N_4 L_s C & N_4 L_s C \end{bmatrix}, \quad \hat{\bar{\mathbb{B}}} = \begin{bmatrix} N_2 L_s C & 0 \\ N_4 L_s C & 0 \end{bmatrix}, \end{aligned}$$

$$\hat{\mathbb{B}}_\epsilon = \hat{\bar{\mathbb{B}}}_g = \begin{bmatrix} N_2 L_s \\ N_4 L_s \end{bmatrix}.$$

To decouple the nonlinear terms  $N_2 L_s$  and  $N_4 L_s$ , (37) is reformed as

$$\mathbb{E}\{\mathbf{Sy}(\Upsilon + \mathbf{He}(\hat{\mathcal{N}}(\hat{\mathcal{G}} + \tilde{\mathcal{G}})), \varphi(t))\} < 0, \quad (38)$$

which is ensured by

$$\begin{aligned} &\Upsilon + \mathbf{He}(\hat{\mathcal{N}}(\hat{\mathcal{G}} + \tilde{\mathcal{G}})) + \mathbf{He}(\hat{\mathcal{N}}\bar{\mathbb{A}}_2\tilde{\mathcal{G}}) \\ &= \Upsilon + \mathbf{He}(\hat{\mathcal{N}}(\hat{\mathcal{G}} + \hat{\mathbb{G}})) + \mathbf{He}(\hat{\mathcal{N}}\bar{\mathbb{A}}_2\tilde{\mathcal{G}}) < 0, \end{aligned} \quad (39)$$

where

$$\begin{aligned} \hat{\mathbb{G}} &= \hat{\bar{\mathbb{A}}}\mathbb{L}_2 - \hat{\bar{\mathbb{B}}} \sum_{j=0}^3 f_j \mathbb{L}_{3+j} + \hat{\bar{\mathbb{B}}}_\epsilon \mathbb{L}_{11} - \beta \hat{\bar{\mathbb{B}}}_g \mathbb{L}_{13}, \\ \tilde{\mathcal{G}} &= \bar{\mathbb{A}}\mathbb{L}_2 - \tilde{\bar{\mathbb{B}}} \sum_{j=0}^3 f_j \mathbb{L}_{3+j} + \tilde{\bar{\mathbb{B}}}_\epsilon \mathbb{L}_{11} - \beta \tilde{\bar{\mathbb{B}}}_g \mathbb{L}_{13}, \\ \bar{\mathbb{A}} &= \begin{bmatrix} L_s C & L_s C \\ L_s C & L_s C \end{bmatrix}, \quad \tilde{\bar{\mathbb{B}}} = \begin{bmatrix} L_s C & 0 \\ L_s C & 0 \end{bmatrix}, \\ \tilde{\bar{\mathbb{B}}}_\epsilon &= \tilde{\bar{\mathbb{B}}}_g = \begin{bmatrix} L_s \\ L_s \end{bmatrix}. \end{aligned}$$

According to Lemma 1, one has

$$\begin{bmatrix} \Upsilon + \mathbf{He}(\hat{\mathcal{N}}(\hat{\mathcal{G}} + \hat{\mathbb{G}})) & \hat{\mathcal{N}}\bar{\mathbb{A}}_2 + \mu(\bar{\mathbb{A}}_1\tilde{\mathcal{G}})^\top \\ * & -\mu\mathbf{He}(\bar{\mathbb{A}}_1) \end{bmatrix} < 0, \quad (40)$$

By defining new variable  $\mathcal{L}_s = XL_s$  and substituting it into (40), the condition (36) in Theorem 2 is obtained. Then the proof is fulfilled. ■

*Remark 5:* Compared with the existing method requiring  $N_2 = N_4$  to design estimator and filter gains, a slack variable  $X$  introduced by using Lemma 1 is applied to separate the coupled terms  $N_2 L_s C$  and  $N_4 L_s C$ . According to this operation, the special structural constraint of matrix  $\mathbf{N}$  is removed. This indicates that the obtained conditions in Theorem 2 are less conservative than the corresponding results derived by using the existing method [24].

#### IV. SIMULATION RESULTS

*Example 1.*

In the example, we consider the same parameters with [23] and [29] as:

$$\begin{aligned} \mathcal{N}_1 &= 0.5263, & \mathcal{N}_2 &= 0.4211, & \mathcal{M}_1 &= -0.0103, \\ \mathcal{M}_2 &= -0.0202, & \mathcal{M}_3 &= 0.0380, & \mathcal{M}_4 &= 0.798, \\ \mathcal{M}_5 &= -0.46, & \nu &= 1.63, & \kappa &= 2.084. \end{aligned}$$

The gain  $\mathcal{K} = [1.118 \ 3.465 \ 6.6327 \ -1.5691 \ 3.1662]$  is taken to render the system to be stable. Then, some other matrices are set as

$$\begin{aligned} G &= 0.3, \quad C = [0 \ 0.5 \ 1 \ 2 \ 0.5], \\ D &= [1 \ 0 \ 1 \ 0 \ 0]. \end{aligned}$$

To demonstrate the advantage of the proposed FETM than the existing methods, two comparison cases are simulated as follows.

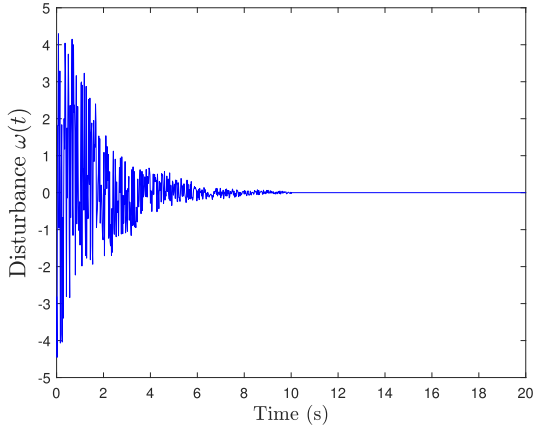
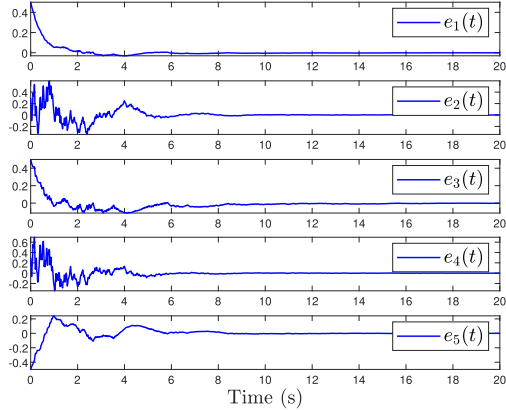
Fig. 3. The curves of external disturbance  $\omega(t)$ .

Fig. 4. The state responses of the estimating error system under the normal ETM (7) in [22].

#### A. The First Comparison Case

**First**, without considering measurement outliers, the comparison of FETM (5) and existing normal ETM (7) in [22] is given. By choosing  $\delta_1 = 0.02$ ,  $\delta_2 = \infty$ ,  $\rho_1 = 20$ ,  $\rho_2 = 10$ ,  $\rho_3 = 10$ ,  $\beta = 0.5$ ,  $\bar{\eta} = 0.05$ ,  $\tau = 0.08$ ,  $h = 0.02$ ,  $\gamma = 2$  and solving Theorem 1, the estimator gain and triggering matrix are obtained as

$$\Psi = 1877.9,$$

$$L_s = [-0.2832, -1.5266, -1.3438, -2.8763, 0.2613]^\top.$$

The external disturbance is considered as  $\omega(t) = e^{-0.5t}[\varpi(t) + \sin(0.5\pi t)]$  for  $t \in [0, 10s]$  (otherwise,  $\varpi(t) = 0$ ), where  $\varpi(t)$  is a random variable satisfying  $|\varpi(t)| \leq 5$ . The initial conditions of system and estimator are  $\theta(0) = [2 \ 0.8 \ -1 \ 0.5 \ -1]^T$  and  $\theta_s(0) = [1.5 \ 0.5 \ -1.5 \ 0.2 \ -0.5]^T$ . Following the similar way in [19], the deception attacks are considered as  $g(v(t)) = \tanh(0.3v(t))$ . Then, the curves of external disturbance, the state responses of estimating error  $e(t)$ , the triggering time intervals under our FETM and traditional ETM in [22] are drawn in Fig. 3 - Fig. 7. In TABLE I, the number ( $\mathcal{N}_1$ ) of transmissions and the ratio ( $\mathcal{N}_2$ ) between  $\mathcal{N}_1$  and total sampling data under the two ETMs are compared.

In terms of these figures, it is shown that the designed estimator and FETM can ensure the estimating error system to be asymptotically stable under external disturbances and deception attacks. The convergence time and estimating per-

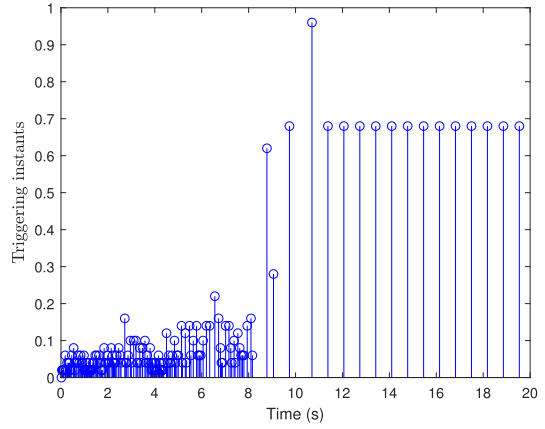


Fig. 5. The triggering instants under normal ETM (7) in [22].

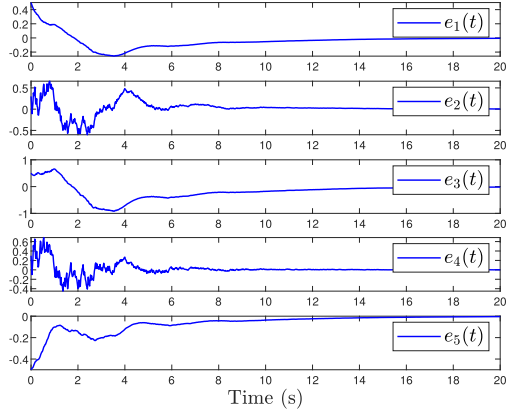


Fig. 6. The state responses of the estimating error system under the proposed FETM (5).

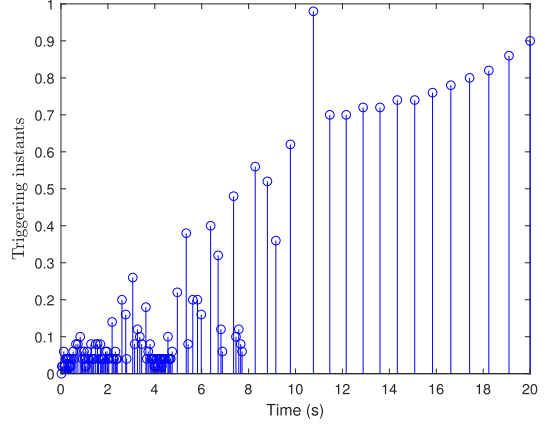


Fig. 7. The triggering instants under the proposed FETM (5).

TABLE I  
THE COMPARISON OF  $\mathcal{N}_1$  AND  $\mathcal{N}_2$  UNDER THE DIFFERENT ETMs WITHOUT MEASUREMENT OUTLIERS

Method	$\mathcal{N}_1$	$\mathcal{N}_2$
Time-triggered sampling	1000	100%
Normal ETM (7) in [22]	165	16.5%
FETM (5)	119	11.9%

formance under our FETM and normal ETM are very similar. Nevertheless, TABLE I indicates that our proposed FETM is effective for reducing the number of triggering times and the waste of limited network resources. The reason is that

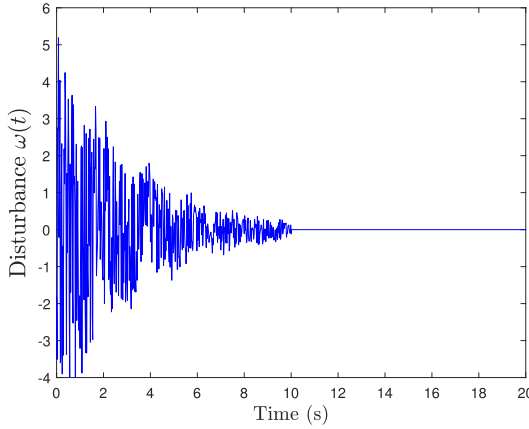
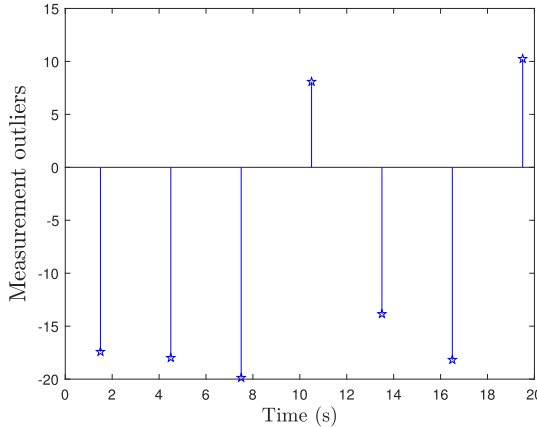
Fig. 8. The curves of external disturbance  $\omega(t)$ .

Fig. 9. The measurement outliers.

the proposed FETM using the historical information is able to restrict the fluctuations induced by stochastic disturbances, which is helpful in reducing some redundant triggering events.

### B. The Second Comparison Case

Second, by considering measurement outliers, the comparison of FETM and conventional ORETM in [13] is executed. The same parameters with the first case, except for  $\delta_1 = 0.05$  and  $\delta_2 = 100$ , are considered to derive the following parameters:

$$\Psi = 547.0069,$$

$$L_s = [0.3132, 1.3467, 1.4599, 1.6784, -0.9660]^\top.$$

The external disturbance is considered as  $\omega(t) = e^{-0.3t}[\varpi(t) + \cos(\pi t)]$  for  $t \in [0, 10s]$  (otherwise,  $\varpi(t) = 0$ ), where  $\varpi(t)$  is a random variable satisfying  $|\varpi(t)| \leq 5$ , which is shown in Fig. 8. The initial conditions and the deception attacks are the same with the first case. The measurement outliers are characterized by a stochastic variable with bound 20 and emerge each 3 seconds starting from  $t = 1.5s$ , which are shown in Fig. 9. Then, the corresponding comparison figures are depicted in Fig. 10 - Fig. 13. The comparison results of  $\mathcal{N}_1$  and  $\mathcal{N}_2$  are derived in TABLE II.

According to these figures, it is seen that both the proposed ETMs are able to remove the signals with measurement outliers to render the estimating error system stable under

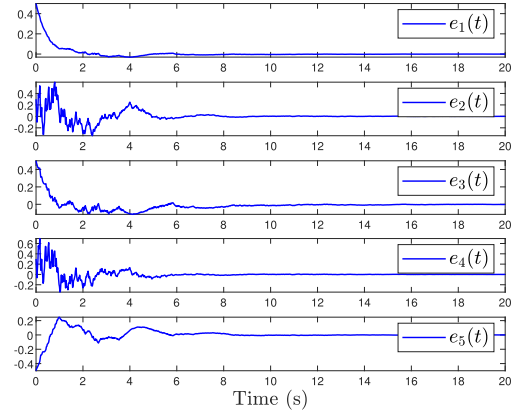


Fig. 10. The state responses of the estimating error system under the ORETM (6) in [13] with measurement outliers.

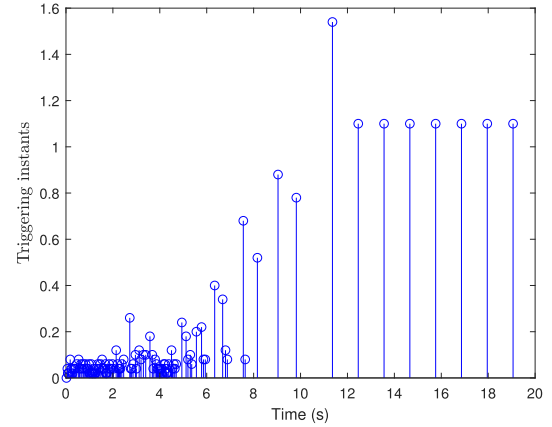


Fig. 11. The triggering instants under the ORETM (6) in [13] with measurement outliers.

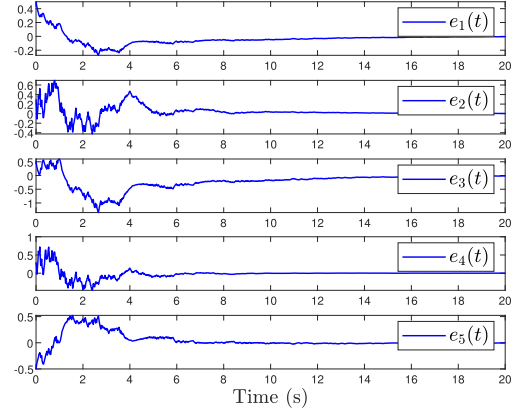


Fig. 12. The state responses of the estimating error system under the proposed FETM (5) with measurement outliers.

TABLE II  
THE COMPARISON OF  $\mathcal{N}_1$  AND  $\mathcal{N}_2$  UNDER THE DIFFERENT ETMs WITH MEASUREMENT OUTLIERS

Method	$\mathcal{N}_1$	$\mathcal{N}_2$
Time-triggered sampling	1000	100%
ORETM (6) in [13]	116	11.6%
FETM (5)	78	7.8%

disturbances and deception attacks. Moreover, compared to the conventional ORETM in [13], the presented FETM-based estimator obtains similar estimating performance with fewer triggering data. To be specific, from TABLE II, the value of

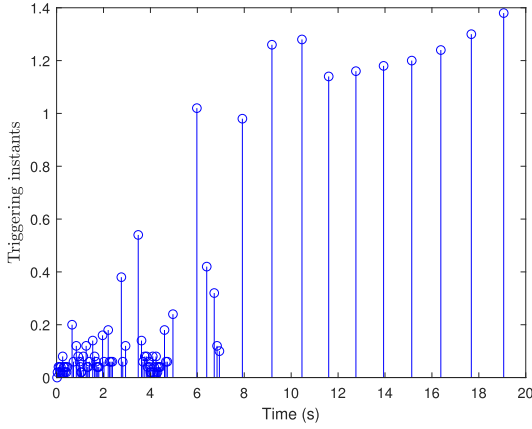


Fig. 13. The triggering instants under the proposed FETM (5) with measurement outliers.

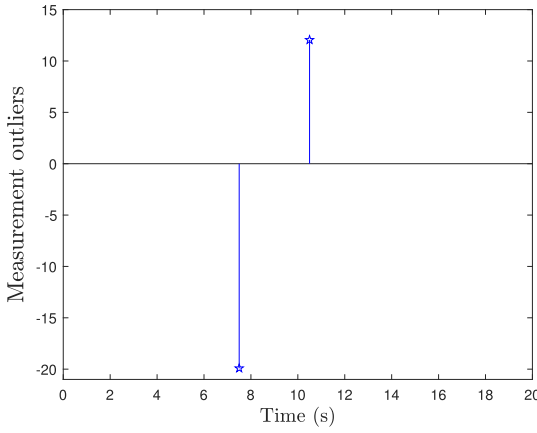


Fig. 14. The measurement outliers.

$\mathcal{N}_1$  obtained by utilizing FETM (5) is dramatically decreased 32.76% compared to the existing ORETM (6) in [13].

### C. The Third Comparison Case

Third, by considering the same measurement outliers in the second case, the comparison of FETM and integral-based ETM in [23] is executed to show the effectiveness of excluding the false triggering events caused by measurement outliers. The same parameters, external disturbance and deception attacks with the second case are considered.

The initial conditions of system and estimator are  $\theta(0) = [3 \ 1 \ -2 \ 1 \ -1]^T$  and  $\theta_s(0) = [1.5 \ 0.5 \ -1.5 \ 0.2 \ -0.5]^T$ . The measurement outliers are characterized by a stochastic variable with bound 20 and emerge at 7.5s and 10.5s, which are drawn in Fig. 14. Then, the corresponding comparison figures about the state responses of estimating error system are depicted in Fig. 15.

Based on the above figures, one observes that when measurement outliers happen, our proposed FETM enables to exclude them and generate better estimating performance than the existing integral-based ETM in [23]. The reason is that the introduced upper bound of triggering error term in our FETM is able to remove the false triggering events induced by outliers.

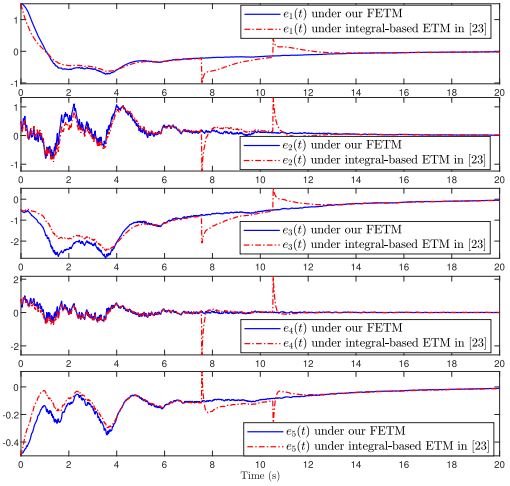


Fig. 15. The state responses of the estimating error system under our FETM and integral-based ETM in [23].

### Example 2.

In the example, we consider the same parameters with [30] as:

$$\begin{aligned} \mathcal{N}_1 &= 0.2308, & \mathcal{N}_2 &= 0.2564, & \mathcal{M}_1 &= -0.0281, \\ \mathcal{M}_2 &= -0.1338, & \mathcal{M}_3 &= 0.468, & \mathcal{M}_4 &= 1.248, \\ \mathcal{M}_5 &= -0.58, & \nu &= 2.2, & \kappa &= 5.866. \end{aligned}$$

The gain  $\mathfrak{K} = [1 \ 3 \ 5 \ -2 \ 4]$  is taken to render the system to be stable. Then, some other matrices are set as

$$\begin{aligned} G &= 0.5, & C &= [1 \ 0 \ 1 \ 0 \ 1], \\ D &= [5 \ 0 \ 4 \ 0 \ 2]. \end{aligned}$$

In the next section, by considering the above cyber-attacks, the comparisons of attack-free case and deception attack case under our designed estimator are executed.

### D. The Fourth Comparison Case

In this case, the same parameters with the second case, except for  $\delta_1 = 0.08$ ,  $\delta_2 = 150$  and  $\gamma = 2.8$ , are considered to derive the following parameters:

$$\Psi = 2316,$$

$$L_s = [0.3783, -0.9185, 0.1326, -0.1235, -0.0704]^\top.$$

The external disturbance is considered as

$$\omega(t) = \begin{cases} e^{-0.5t}[\varpi(t) + 10\sin(\pi t)], & t < 20s \\ e^{-0.25(t-80)}[\varpi(t) + 5\sin(\pi t)], & 80s < t < 120s \\ 0, & \text{otherwise}, \end{cases}$$

where  $\varpi(t)$  is a random variable satisfying  $|\varpi(t)| \leq 20$ , which is drawn in Fig. 16.

In the simulation, the initial conditions and the deception attacks are the same with the first case. The measurement outliers are characterized by a stochastic variable with bound 50 and emerges each 15 seconds starting from  $t = 1.5s$ , which is shown in Fig. 17. Then, the corresponding comparison figures are depicted in Fig. 18.

According to these figures, it is seen that the deception attacks could degrade the estimation performance of the

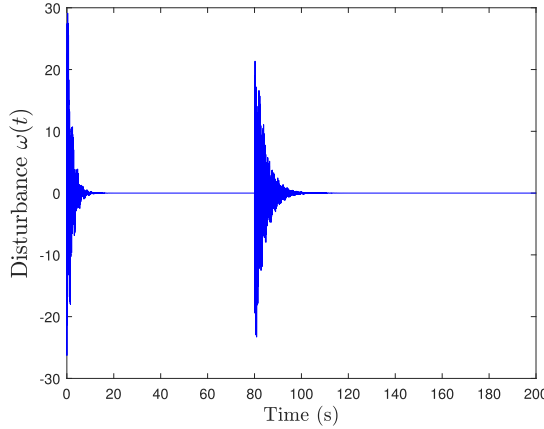


Fig. 16. The curves of external disturbance  $\omega(t)$ .

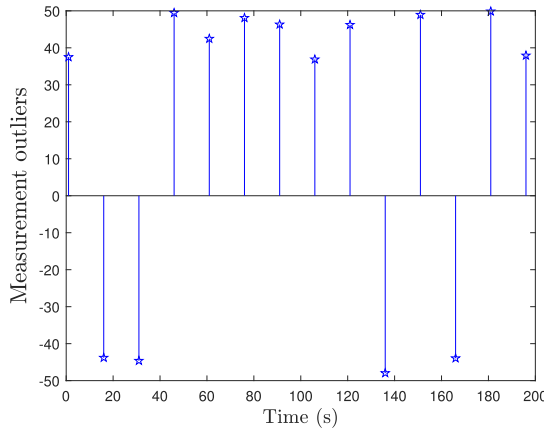


Fig. 17. The measurement outliers.

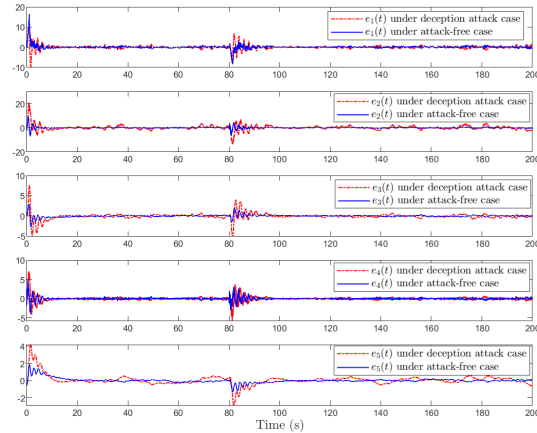


Fig. 18. The state responses of the estimating error system under the attack-free case and deception attack case.

designed estimator. However, the proposed estimator design method is able to guarantee the stability of the estimating error system for both attack-free case and deception attack case. Since the deception attacks are considered in the design of estimator and then it is robust against deception attacks.

## V. CONCLUSION

This paper studied the event-triggered  $H_\infty$  state estimator design of networked ASVs against measurement outliers and deception attacks. To mitigate the communication burden,

a new FETM utilizing the average system outputs was presented to decrease the redundant triggers caused by system disturbances. Moreover, an upper threshold is demanded for the error signal in the triggering condition to reduce the false triggers resulted from measurement outliers. A time-varying delay system was formulated to express the secure event-triggered  $H_\infty$  state estimation error system. Then, some sufficient conditions were obtained for co-designing the estimator gain and the triggering matrix. Lastly, the merits of the developed approach was verified by some simulation results. Moreover, how to extend the developed strategy to deal with the control and state estimator issues of nonlinear ASVs and other nonlinear practical systems needs more investigations in our future work.

## REFERENCES

- [1] Y. Ma, Z. Nie, S. Hu, Z. Li, R. Malekian, and M. Sotelo, "Fault detection filter and controller co-design for unmanned surface vehicles under DoS attacks," *IEEE Trans. Intell. Transp. Syst.*, vol. 22, no. 3, pp. 1422–1434, Mar. 2021.
- [2] Q. Zhang, W. Pan, and V. Reppa, "Model-reference reinforcement learning for collision-free tracking control of autonomous surface vehicles," *IEEE Trans. Intell. Transp. Syst.*, vol. 23, no. 7, pp. 8770–8781, Jul. 2022.
- [3] Y.-L. Wang and Q.-L. Han, "Network-based fault detection filter and controller coordinated design for unmanned surface vehicles in network environments," *IEEE Trans. Ind. Informat.*, vol. 12, no. 5, pp. 1753–1765, Oct. 2016.
- [4] L. Hu et al., "A multiobjective optimization approach for COLREGs-compliant path planning of autonomous surface vehicles verified on networked bridge simulators," *IEEE Trans. Intell. Transp. Syst.*, vol. 21, no. 3, pp. 1167–1179, Mar. 2020.
- [5] S. Yan, Z. Gu, J. H. Park, and X. Xie, "Sampled memory-event-triggered fuzzy load frequency control for wind power systems subject to outliers and transmission delays," *IEEE Trans. Cybern.*, vol. 53, no. 6, pp. 4043–4053, Dec. 2023.
- [6] D. Shah, M. M. D. Santos, H. Chaoui, and J. F. Justo, "Event-triggered non-switching networked sliding mode control for active suspension system with random actuation network delay," *IEEE Trans. Intell. Transp. Syst.*, vol. 23, no. 7, pp. 7521–7534, Jul. 2022.
- [7] F. Yang and X. Song, "Finite-time control for connected vehicles under denial-of-service attacks: A dynamic event-triggered control strategy," *IEEE Access*, vol. 10, pp. 106005–106016, 2022.
- [8] S. Yan, Z. Gu, J. H. Park, and X. Xie, "Adaptive memory-event-triggered static output control of T-S fuzzy wind turbine systems," *IEEE Trans. Fuzzy Syst.*, vol. 30, no. 9, pp. 3894–3904, Sep. 2022.
- [9] Z. Gu, T. Yin, and Z. Ding, "Path tracking control of autonomous vehicles subject to deception attacks via a learning-based event-triggered mechanism," *IEEE Trans. Neural Netw. Learn. Syst.*, vol. 32, no. 12, pp. 5644–5653, Dec. 2021.
- [10] Y. Ma, Z. Nie, Y. Yu, S. Hu, and Z. Peng, "Event-triggered fuzzy control of networked nonlinear underactuated unmanned surface vehicle," *Ocean Eng.*, vol. 213, Oct. 2020, Art. no. 107540.
- [11] Z. Peng, J. Wang, D. Wang, and Q.-L. Han, "An overview of recent advances in coordinated control of multiple autonomous surface vehicles," *IEEE Trans. Ind. Informat.*, vol. 17, no. 2, pp. 732–745, Feb. 2021.
- [12] J. Li, Z. Wang, H. Dong, and G. Ghinea, "Outlier-resistant remote state estimation for recurrent neural networks with mixed time-delays," *IEEE Trans. Neural Netw. Learn. Syst.*, vol. 32, no. 5, pp. 2266–2273, May 2021.
- [13] X. Zhao, C. Liu, J. Liu, and E. Tian, "Probabilistic-constrained reliable  $H_\infty$  tracking control for a class of stochastic nonlinear systems: An outlier-resistant event-triggered scheme," *J. Franklin Inst.*, vol. 358, no. 9, pp. 4741–4760, Jun. 2021.
- [14] J. P. Farwell and R. Rohozinski, "Stuxnet and the future of cyber war," *Survival*, vol. 53, no. 1, pp. 23–40, Feb. 2011.
- [15] H. Liang, Z. Zhang, and C. K. Ahn, "Event-triggered fault detection and isolation of discrete-time systems based on geometric technique," *IEEE Trans. Circuits Syst. II, Exp. Briefs*, vol. 67, no. 2, pp. 335–339, Feb. 2020.

- [16] K. Ding, Y. Li, D. E. Quevedo, S. Dey, and L. Shi, "A multi-channel transmission schedule for remote state estimation under DoS attacks," *Automatica*, vol. 78, pp. 194–201, Apr. 2017.
- [17] Y. Liu and G.-H. Yang, "Event-triggered distributed state estimation for cyber-physical systems under DoS attacks," *IEEE Trans. Cybern.*, vol. 52, no. 5, pp. 3620–3631, May 2022, doi: 10.1109/TCYB.2020.3015507.
- [18] R. Merco, F. Ferrante, and P. Pisu, "A hybrid controller for DOS-resilient string-stable vehicle platoons," *IEEE Trans. Intell. Transp. Syst.*, vol. 22, no. 3, pp. 1697–1707, Mar. 2021.
- [19] L. Hu, Z. Wang, Q.-L. Han, and X. Liu, "State estimation under false data injection attacks: Security analysis and system protection," *Automatica*, vol. 87, pp. 176–183, Jan. 2018.
- [20] Y. Chen, X. Meng, Z. Wang, and H. Dong, "Event-triggered recursive state estimation for stochastic complex dynamical networks under hybrid attacks," *IEEE Trans. Neural Netw. Learn. Syst.*, vol. 34, no. 3, pp. 1465–1477, Mar. 2023, doi: 10.1109/TNNLS.2021.3105409.
- [21] S. Yan, Z. Gu, and J. H. Park, "Memory-event-triggered  $H_\infty$  load frequency control of multi-area power systems with cyber-attacks and communication delays," *IEEE Trans. Netw. Sci. Eng.*, vol. 8, no. 2, pp. 1571–1583, Apr. 2021.
- [22] J. Liu, T. Yin, M. Shen, X. Xie, and J. Cao, "State estimation for cyber-physical systems with limited communication resources, sensor saturation and denial-of-service attacks," *ISA Trans.*, vol. 104, pp. 101–114, Sep. 2020.
- [23] X. Wang, Z. Fei, H. Gao, and J. Yu, "Integral-based event-triggered fault detection filter design for unmanned surface vehicles," *IEEE Trans. Ind. Informat.*, vol. 15, no. 10, pp. 5626–5636, Oct. 2019.
- [24] M. Shen, D. Ye, and Q.-G. Wang, "Mode-dependent filter design for Markov jump systems with sensor nonlinearities in finite frequency domain," *Signal Process.*, vol. 134, pp. 1–8, May 2017.
- [25] A. Selivanov and E. Fridman, "Event-triggered  $H_\infty$  control: A switching approach," *IEEE Trans. Autom. Control*, vol. 61, no. 10, pp. 3221–3226, Dec. 2016.
- [26] K. E. Atkinson, *An Introduction to Numerical Analysis*, 2nd ed. New York, NY, USA: Wiley, 2008.
- [27] X.-H. Chang and G.-H. Yang, "Nonfragile  $H_\infty$  filtering of continuous-time fuzzy systems," *IEEE Trans. Signal Process.*, vol. 59, no. 4, pp. 1528–1538, Apr. 2011.
- [28] P. Park, J. W. Ko, and C. Jeong, "Reciprocally convex approach to stability of systems with time-varying delays," *Automatica*, vol. 47, no. 1, pp. 235–238, Jan. 2011.
- [29] S. Yan, Z. Gu, and C. K. Ahn, "Memory-event-triggered  $H_\infty$  filtering of unmanned surface vehicles with communication delays," *IEEE Trans. Circuits Syst. II, Exp. Briefs*, vol. 68, no. 7, pp. 2463–2467, Jul. 2021.
- [30] Z. Zhou, M. Zhong, and Y. Wang, "Fault diagnosis observer and fault-tolerant control design for unmanned surface vehicles in network environments," *IEEE Access*, vol. 7, pp. 173694–173702, 2019.



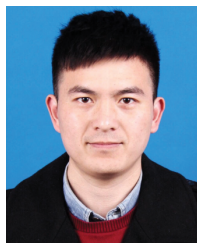
**Zhou Gu** (Senior Member, IEEE) received the B.S. degree in automation from North China Electric Power University, Beijing, China, in 1997, and the M.S. and Ph.D. degrees in control science and engineering from the Nanjing University of Aeronautics and Astronautics, Nanjing, China, in 2007 and 2010, respectively.

From September 1999 to January 2013, he was with the School of Power Engineering, Nanjing Normal University, as an Associate Professor. He was a Visiting Scholar with Central Queensland University, Rockhampton, QLD, Australia; and The University of Manchester, Manchester, U.K. He is currently a Professor with the School of Electrical Engineering, Anhui Polytechnic University, Wuhu, China. He is also a Professor with Nanjing Forestry University, Nanjing. His current research interests include networked control systems, time-delay systems, and reliable control and their applications.



**Ju H. Park** (Senior Member, IEEE) received the Ph.D. degree in electronics and electrical engineering from the Pohang University of Science and Technology (POSTECH), Pohang, Republic of Korea, in 1997. From May 1997 to February 2000, he was a Research Associate with the Engineering Research Center and the Automation Research Center, POSTECH. He joined Yeungnam University, Gyeongsan-si, Republic of Korea, in March 2000, where he is currently the Chuma Chair Professor. He is the coauthor of the monographs *Recent Advances in Control and Filtering of Dynamic Systems with Constrained Signals* (New York, NY, USA: Springer-Nature, 2018) and *Dynamic Systems With Time Delays: Stability and Control* (New York, NY, USA: Springer-Nature, 2019). His research interests include robust control and filtering, neural/complex networks, fuzzy systems, multiagent systems, and chaotic systems. He has published a number of articles in these areas.

He is a fellow of the Korean Academy of Science and Technology (KAST). Since 2015, he has been a recipient of the Highly Cited Researchers Award by Clarivate Analytics (formerly, Thomson Reuters) and listed in three fields, engineering, computer sciences, and mathematics in 2019 and 2022. He is an Editor of an edited volume *Recent Advances in Control Problems of Dynamical Systems and Networks* (New York: Springer-Nature, 2020). He is also a Subject Editor/Advisory Editor/Associate Editor/Editorial Board Member of several international journals, including *IET Control Theory & Applications*, *Applied Mathematics and Computation*, *The Journal of the Franklin Institute*, *Nonlinear Dynamics, Engineering Reports*, *Cogent Engineering*, *IEEE TRANSACTIONS ON FUZZY SYSTEMS*, *IEEE TRANSACTIONS ON NEURAL NETWORKS AND LEARNING SYSTEMS*, and *IEEE TRANSACTIONS ON CYBERNETICS*.



**Shen Yan** received the B.E. degree in automation and the Ph.D. degree in power engineering automation from Nanjing Technology University, Nanjing, China, in 2014 and 2019, respectively.

From November 2017 to November 2018, he was a Visiting Ph.D. Student with the University of Auckland, Auckland, New Zealand. From February 2022 to August 2022, he was a Visiting Scholar with Yeungnam University, Gyeongsan-si, Republic of Korea. He is currently an Associate Professor with the College of Mechanical and Electronic Engineering, Nanjing Forestry University, Nanjing. His current research interests include networked control systems and event-triggered control and their applications.



**Mouquan Shen** received the Ph.D. degree in control theory and control engineering from the College of Information Science and Engineering, Northeastern University, Shenyang, China, in 2011.

He is currently a Professor with the College of Electrical Engineering and Control Science, Nanjing Technology University, Nanjing, China. He is also with the Department of Electrical Engineering, Yeungnam University, Gyeongsan-si, Republic of Korea. His current research interests include Markov jump systems, adaptive control, data-driven-based control, robust control, and interactive learning control.